



A simplified microwave-based motion detector for home cage activity monitoring in mice

Andreas Genewsky^{1*} , Daniel E. Heinz^{1,2}, Paul M. Kaplick^{1,3,4}, Kasyoka Kilonzo^{1,5} and Carsten T. Wotjak¹

Abstract

Background: Locomotor activity of rodents is an important readout to assess well-being and physical health, and is pivotal for behavioral phenotyping. Measuring homecage-activity with standard and cost-effective optical methods in mice has become difficult, as modern housing conditions (e.g. individually ventilated cages, cage enrichment) do not allow constant, unobstructed, visual access. Resolving this issue either makes greater investments necessary, especially if several experiments will be run in parallel, or is at the animals' expense. The purpose of this study is to provide an easy, yet satisfying solution for the behavioral biologist at novice makers level.

Results: We show the design, construction and validation of a simplified, low-cost, radar-based motion detector for home cage activity monitoring in mice. In addition we demonstrate that mice which have been selectively bred for low levels of anxiety-related behavior (LAB) have deficits in circadian photoentrainment compared to CD1 control animals.

Conclusion: In this study we have demonstrated that our proposed low-cost microwave-based motion detector is well-suited for the study of circadian rhythms in mice.

Keywords: Home cage activity monitoring, Arduino, DIY, Open-source, Doppler-shift, Radar

Background

The monitoring of circadian rhythms in laboratory mice is essential in biomedical research and goes far beyond the issues of chronobiology. Numerous psychiatric illnesses are comorbid with sleep/circadian disturbances [1] rendering the assessment of rodent locomotor activity an important measure in pre-clinical psychiatric research. Mouse models of psychiatric disorders have been found to be ethological valid [2] with respect to changes in circadian rhythms e.g. trait-anxiety [3] and also social-stress induced depression-like behavior [4]. However, the trend to replace conventional open-top with individually-ventilated cages as well as increasing use of environmental enrichment (e.g. wooden tunnels), hinder the function of the well-proven optical based methods as visual access is obstructed. Disproportional financial expenditure for

special cages and apparatuses are necessary to implement this formerly rather simple behavioral phenotyping test. Therefore it is not surprising, that the normalized numbers of publications using the term 'locomotor activity', 'home cage activity' or 'circadian rhythm' are regressive [5]. Conventional methods to measure home cage activity in small rodents are typically based on vibration/tilt sensing [6–8], infrared light beam crossings [9], resistance changes [10], capacitive sensing [11], video tracking [12], wheel-running [13], passive infrared emission [14], ultrasound transducers [15] but also microwave-based Doppler-shift radar systems [16–20]. Since each of these methods has its own advantages and disadvantages, we wanted our hardware to meet the following criteria: (a) flexible usage with various cage types, (b) simple, standalone operation and fast access to raw data, (c) motion detection without visual contact to the animal, (d) fast detection <1 Hz sampling rate, (e) open-source, and cost-effective, (f) easy to build with readily available tools. Here we present the design, construction and validation of a simplified microwave-based Doppler shift

*Correspondence: andreas_genewsky@psych.mpg.de

¹Max Planck Institute of Psychiatry, Dep. Stress Neurobiology and Neurogenetics, RG Neuronal Plasticity, Kraepelinstr. 2-10, D-80804 Munich, Germany

Full list of author information is available at the end of the article

motion detector, with emphasis on detailed and comprehensive building instructions. Further we have applied the proposed system to assay circadian rhythmicity and photoentrainment in a mouse model which was initially established to resemble a low anxiety-related behavior (LAB) phenotype [21]. However, those animals have been found in addition to mimic certain characteristics of attention deficit hyperactivity disorder (ADHD) [22], including increased locomotor activity in emotionally challenging behavioral tasks as well as a slightly disturbed sleeping pattern [23]. We could demonstrate that LAB animals show a drastically increased homecage locomotor activity and additionally suffer from deficits in photoentrainment.

Methods

Animals

In this study only male LAB [21] ($N = 3$) and CD1 ($N = 4$) mice have been used. Both strains were bred in the animal facilities of the Max Planck Institute of Psychiatry, Munich, Germany. The selective breeding of LAB animals has been described extensively elsewhere [21, 22]. All animals have been single-housed >1 week prior to the experiments in Makrolon type II cages ($23 \times 16.5 \times 14$ cm) equipped with wood chip bedding and nesting material (wood wool). The animals were kept under standard housing conditions: 12h/12h inverted light-dark cycle (light off at 8 AM), temperature 24°C, food and water *ad libitum*. Experimental procedures involving animals were approved (AZ 188-12) by the Committee on Animal Health and Welfare of the State of Bavaria (Regierung von Oberbayern, Munich, Germany). Animal care taking and experiments were performed in compliance with the European Economic Community (EEC) directive on the protection of animals used for scientific purposes (2010/63/EU).

PCB design & manufacturing

The printed circuit boards (PCBs) have been designed using the cross-platform open-source electronic design automation suite KiCAD [24]. All design files are available online [25] or on request. The PCBs have been manufactured by the community printed circuit board service OSH Park [26] using the standard manufacturing parameters: two-layered FR4, 1.6 mm thickness, electroless nickel immersion gold finish, clearance >160 μm , trace width >160 μm , >254 μm drill size. The circuit board however is rather simple (e.g. stray capacitances can be largely neglected) and a DIY solution using presensitized PCBs, UV exposure, fixation and etchants like iron(III) chloride or hydrogen peroxide/hydrochloric acid give very good results. An entire assembly using per-board likely requires wired components, instead of the surface-mounted devices (SMD).

Software design

The cross-platform software to write and upload the Arduino code (*see* Listing 1, [Additional file 1]) is freely available online [27]. All files (including the raw data used for this publication) are available online [25] or on request. The Python analysis script (*see* Listing 2) [Additional file 1] was written using Anaconda Python 3.5 [28]. Porting this script to Octave, MATLAB or C++ is possible with only little effort.

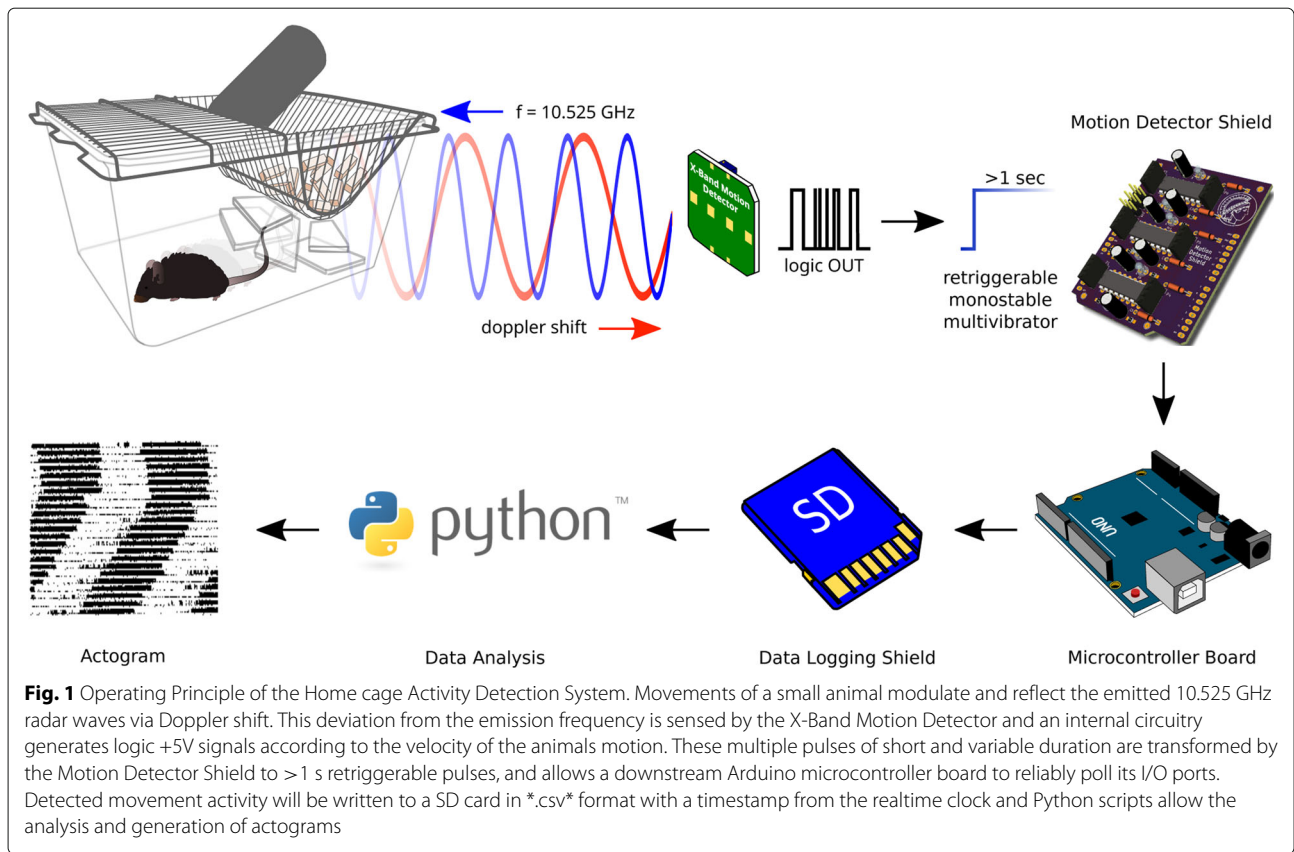
Statistical analysis

All data is presented as mean values \pm standard error. Statistical analysis has been performed using GraphPad Prism 5.03. One-way and two-way analysis of variance was followed by *Dunnett's Multiple Comparison Test* or *Bonferroni* post-hoc analysis. Pearson correlation coefficients were determined using the Scipy function *pearsonr()* included the *stats* module.

Results

Operating principle and circuit design

The overview of the operating principle of microwave-based homecage-activity monitoring system is depicted in Fig. 1. The X-Band Motion Detector module (Parallax Inc, #32213) emits electromagnetic waves at a frequency of 10.525 GHz [29], pulsed at 1.34 kHz with 25 μs pulse duration (measured). These microwaves penetrate through the cage walls, bedding and housing material but are partly reflected by the animal. The frequency of the reflected waves is modulated due to the Doppler shift which allows the X-Band Motion Detector module to capture movement and output logic +5 volt signals as a function of the animals velocity. In order to reliably detect movement across up to six inputs, another interface board, the Motion Detector Shield (MDS) is necessary. Each logic output from up to six X-Band Motion Detectors is fed into three dual, monostable, retriggerable multivibrators (SN74LS423), which transform the short pulses in the microsecond range, to pulses of at least 1 s. This is sufficient for the Arduino microcontroller board to poll the digital inputs for the state. Additionally the Motion Detector Shield possesses an onboard ambient light sensor (TEMT6009) which allows to capture the light intensity. Present on the shield are three additional general purpose input/outputs pins (GPIO) or 10-bit analog-to-digital converters (ADC) in a convenient (+5V-GND-SIGNAL) three-pin configuration, which allows the easy connection of other sensors (e.g. an electret microphone) or switches. After every detected movement a short latency <5 μs interrupt is generated which initiates the polling and data handling routines. After the data has been written to the SD card via the Data Logger Shield (Adafruit Industries, LLC, #1141) the multivibrators are reset, allowing the circuit to react again to new incoming



movement events. The data is stored as standard comma-separated values (*.csv*) and easily accessible with various open-source spreadsheet programs like Gnumeric or LibreOffice Calc rendering our system cross-platform capable. However, simple scripts written in Python 3.5 [28] allow a quick and flexible standardized high quality analysis. The outputs from the X-Band Motion Detector modules are connected to the MDS via the pin headers P1-P6 and are summed first altogether through the diodes D1-D6 and routed to one of the Arduino's interrupt pin. Additionally, the sensor outputs are routed to the multivibrators (IC1-IC3) where the RC circuits consisting of C1-C6 and R4-R7, R11, R12 generate >1 s pulses. These pulses are available at the Arduino's digital inputs pin after an interrupt has been sensed by the interrupt function *detected()* (see Listing 1) [Additional file 1], all inputs flopA-flopF will be polled, the result will be written to the sensors [] array and the state variable changes (to HIGH). In the subsequent loop, the main function will see the if() condition fulfilled and writes the sensor[] array together with the timestamp from the RTC to the SD card. Afterwards flopRST will be pulled down briefly whereby all multivibrators are reset. Every motion event is signaled with a red (>640 nm) LED, which is only barely visible to mice and rats [30–32]. In order to completely exclude any disturbances due to the red light flashes, we

recommend to cover the motion detector shield during recording (e.g. with a cardboard box) or alternatively place it outside of the recording setup. The MDS is stacked together with the Data Logger Shield onto an Arduino Uno Rev.3 microcontroller board (see Fig. 2b). The components used in this design are readily available (see Table 1) and easy to hand-solder. All diodes, capacitors, connectors and integrated circuits are through-hole components, whereas the resistors are easy to handle SMD 0805 packages. The printed circuit boards were manufactured by OSH Park [26]. The design files for the MDS (see Fig. 2c and e) can be directly accessed online [25] or are available upon request. The last step is to upload the code from listing 1 (*motion.ino*) [Additional file 1] in the standard way described here [33]. In order to compile the code the libraries 'SD.h', 'RTCLib.h' and 'Wire.h' need to be installed using the Arduino IDE Library Manager. In order to use the motion detector modules in close range (e.g. type II mouse cages), we need to replace the original potentiometer with at least 50-100 kΩ as suggested previously [20]. The potentiometer is removed with rather 'brute force' using a large enough wire cutter (see Fig. 2e). After cleaning the solder points with fresh solder the SMD resistors RI and RII can be applied as seen in Fig. 2f. This leads to a rather sensitive setup and electrical shielding using aluminum foil in between the cages is

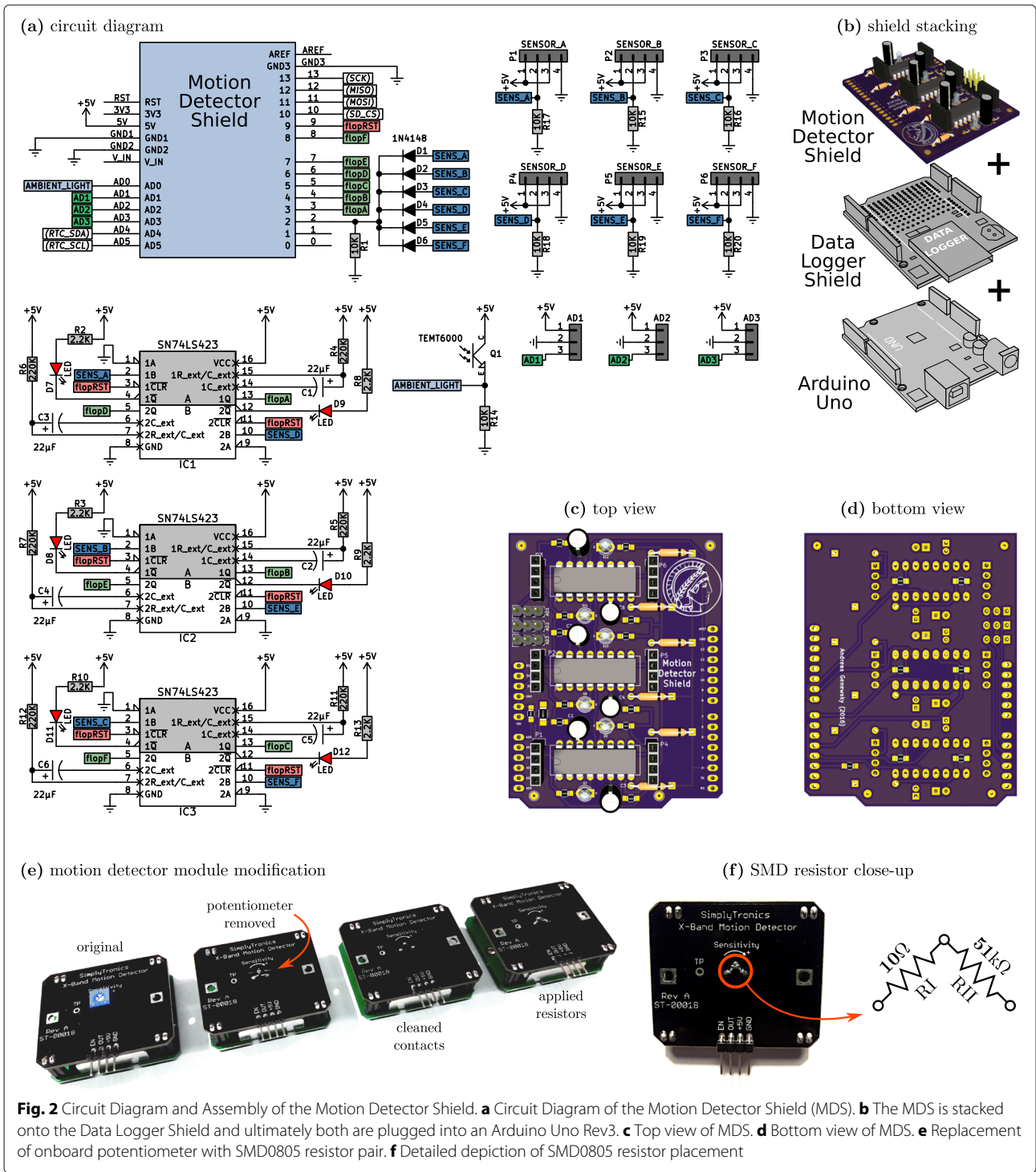


Fig. 2 Circuit Diagram and Assembly of the Motion Detector Shield. **a** Circuit Diagram of the Motion Detector Shield (MDS). **b** The MDS is stacked onto the Data Logger Shield and ultimately both are plugged into an Arduino Uno Rev3. **c** Top view of MDS. **d** Bottom view of MDS. **e** Replacement of onboard potentiometer with SMD0805 resistor pair. **f** Detailed depiction of SMD0805 resistor placement

necessary. Optionally the resistor RII can be replaced with 100 kΩ. The current consumption of the entire system (six sensors attached, all LEDs lighting up, writing data to the SD card) was maximally 180 mA and typically 135 mA, while being powered from a 12 V, 500 mA wall-wart type linear DC power supply. The current consumption of a single enabled X-Band Motion Detector module was 6.3

mA at 5.00 V. For applications where high levels of locomotor activity are expected, we therefore recommend to operate the purposed design using mains power. Another important issue is the potentially hazardous exposure to microwave radiation. According to data sheet [29] the X-Band Motion Detector modules are designed to meet the FCC rules for use within a building [34] and it is

Table 1 List of materials for the motion detector shield

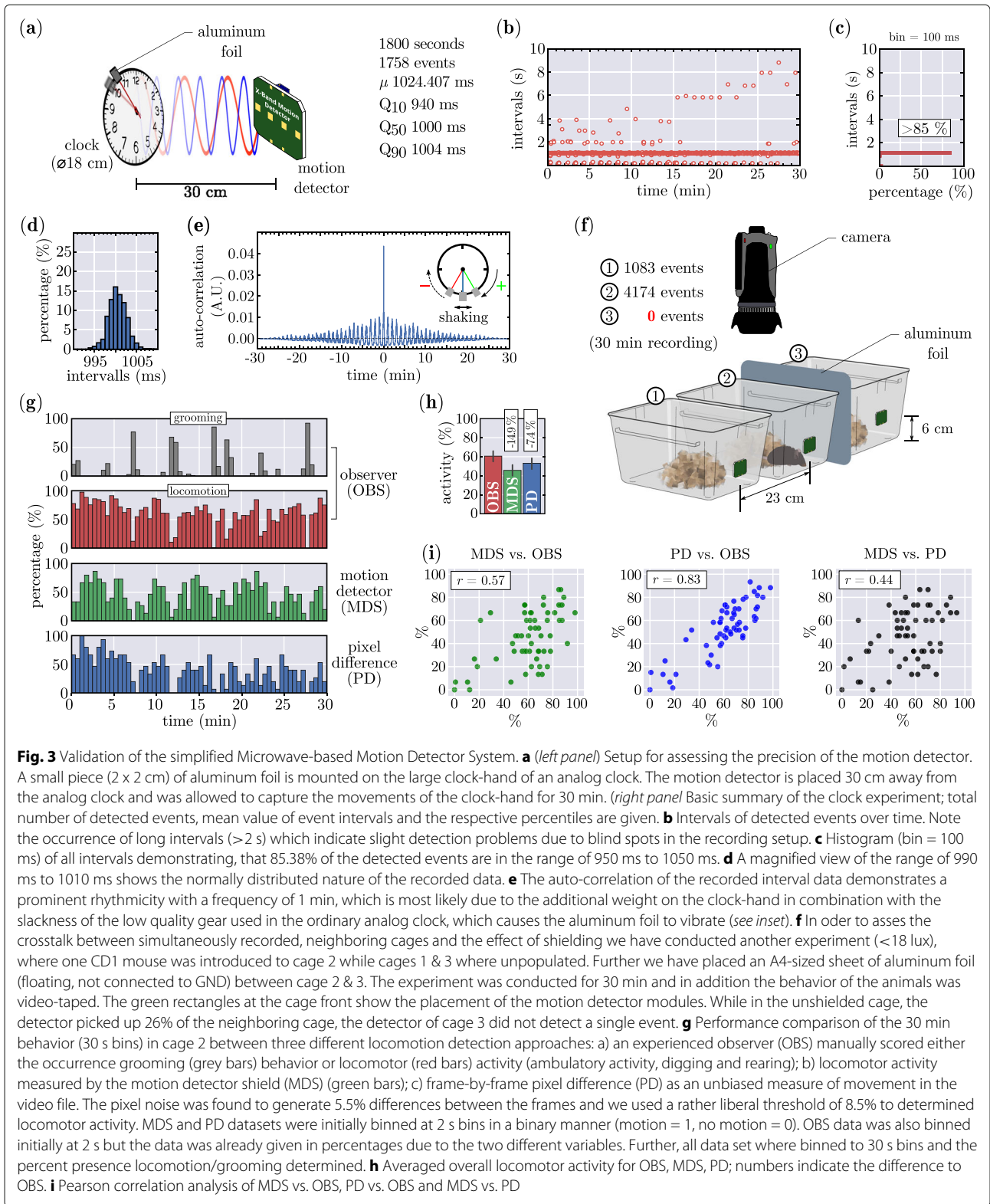
Reference	Qty.	Item	Part No.	Mfr.	RS No.
AD1, AD2, AD3	3	3-pole, 2.54 mm, header	M20-9990346	Harwin	745-7068
C1, C2, C3, C4, C5, C6	6	electrolytic capacitor 22 μ F, 25V	ECE-A1EKA220	Panasonic	807-3554
D1, D2, D3, D4, D5, D6	6	1N4148, 100V, 300mA	1N4148	Fairchild Semi	843-1562
D7, D8, D9, D10, D11, D12	6	LED, 3 mm, 1.85V, red	L-7104SRC-D	Kingbright	619-4886
IC1, IC2, IC3	3	SN74LS423N	SN74LS423N	Texas Instr.	809-5661
P1, P2, P3, P4, P5, P6	6	4-pole, 2.54 mm, socket	M20-7820446	Harwin	681-6814
Q1	1	TEMT6000 Light Sensor	TEMT6000X01	Vishay	768-9354
R1, R14, R15, R16, R17, R18, R19, R20	8	10 k Ω , SMD 0805	CRG0805F10K	TE Connect.	223-0562
R2, R3, R8, R9, R10, R13	6	2.2 k Ω , SMD 0805	CRG0805F2K2	TE Connect.	223-0477
R4, R5, R6, R7, R11, R12	6	220 k Ω , SMD 0805	CRG0805F220K	TE Connect.	223-0742
–	6	X-Band Motion Detector SimplyTronics	32213	Parallax Inc.	781-3074
–	6	4-pole, female, 2.54 mm	5-103960-3	TE Connect.	842-8021
–	6	4-pole, male, 2.54 mm	5-103944-3	TE Connect.	842-8093
–	1	PTFE Cable	–	RS Pro	877-5443
–	2	Arduino Stackable Header Kit - R3	PRT-11417	Sparkfun	–
–	1	Data Logger Shield	1141	Adafruit	–
–	1	Arduino Uno Rev3	A000073	Arduino	769-7409
RI	6	10 Ω , SMD 0805	CRG0805F10R	TE Connect.	223-0152
RII	6	51 k Ω , SMD 0805	CRCW080551K0FKEA	Vishay	679-1525
–	1	DC power supply	8154014	RS Pro	737-8149

further stated that the microwave emissions are below established safety standards for general public environments [35].

Validation of the simplified microwave-based motion detector system

Besides the easy assembly and simple usage, the most important hallmark of our design is the good temporal precision. We have used an analog clock [20] with a piece (2 x 2 cm) of aluminum foil attached to the second clock hand (see Fig. 3a). The motion detector was placed 30 cm away from the clock and allowed to record the clock-hand movements for 30 min (1800 s). During the recording session the system detected 1758 events with a median value of 1.000 s and an average of 1.02407 s (see Fig. 3a

right panel). Figure 3b shows the intervals in between the detected motion events and notably, besides high overall accuracy, there are several intervals which fall well outside the 1 s range. These events cannot be attributed to a potential malfunction of the MDS but stem from the certainly amendable measurement setup. A quantification of the events (Fig. 3c) reveals that 85.38% of all intervals fall into the 950-1050 ms range. A closer look at the the intervals between 990-1010 ms (Fig. 3d) shows the normally distributed nature of the measured data. In order to test, whether our movement detection approach is qualified and sufficiently sensitive to detect rhythmic changes, we utilized the rather poor quality of the analog clock-work. An auto-correlation (Fig. 3e) of the interval data shows the rhythmic modulation of the data every minute.



This is most likely due to the additional weight on the clock-hand in combination with the slackness in the clock-work which causes the aluminum foil to shake (see Fig. 3e

inset). To determine the amount of shielding necessary to eliminate any crosstalk between to neighboring cages which are simultaneously measured with the MDS, we

have conducted the experiment outlined in Fig. 3f. Three cages (with bedding and nesting material) were placed close to each other, and every cage was equipped with a motion detector module (green rectangles) using double-sided tape. Between cage 2 & 3 we have introduced an A4-sized piece of aluminum foil (floating, not connected to GND) and only cage 2 contained a CD1 animal, whose activity was monitored for 30 min at dim illumination (<180 lux). While in the unshielded but unpopulated cage the motion detector picked up 26% of the neighboring cage, the aluminum foil effectively eliminated any crosstalk. In the same experiment we have in addition used a video camera to record the animals motion and an experienced observer manually scored the occurrence of grooming behavior as well as locomotion, which we defined as ambulatory activity, digging and rearing. From the video file we further deduced the frame-by-frame absolute pixel difference and used the number of changed pixels as an unbiased measure of motion in the video. This allowed a performance comparison of the three different approaches shown in Fig. 3g. Notably both, the motion detector (MDS) and the pixel difference (PD) approach, equally reliably detect the absence of locomotor activity during high levels of grooming as well as high levels of locomotion. However, differences in the total amount of detected locomotor activity exist between the three methods (Fig. 3h), where the PD approach resulted in 7.4% less activity compared to the human observer, the MDS approach detected 14.9% less than OBS. Pearson correlation analysis (Fig. 3i) revealed a moderate positive correlation between the MDS and OBS (Pearson's $r = 0.57$), a high positive correlation between PD and OBS (Pearson's $r = 0.83$) and a low positive correlation between MDS and PD (Pearson's $r = 0.44$).

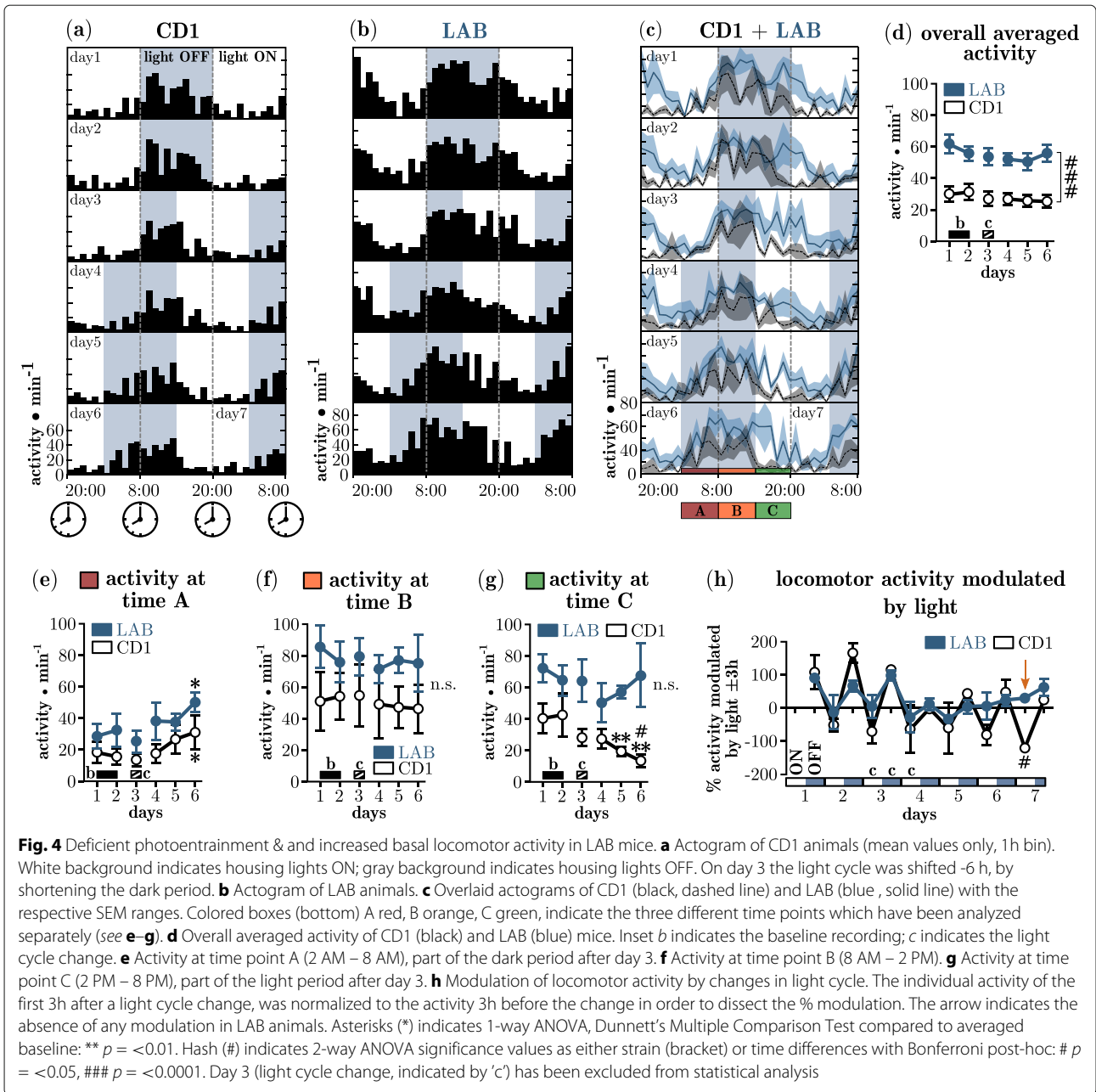
Altered circadian photoentrainment and locomotor activity in LAB mice

In order to test whether our system is able to detect the activity changes in two different mouse lines, we have made use of the low-anxiety related behaving animals (LAB mice) which were also described as a model for attention deficit hyperactivity disorder (ADHD) and were shown previously to display increased activity in emotionally challenging behavioral tasks [21, 22]. Before the onset of the experiment, the animals were kept at an inverted 12h/12h light-dark cycle (8:00PM light ON, 8:00AM light OFF) for 1 week, which was shifted minus 6h (advance) at day 3. The photoentrainment of the circadian rhythm allows the animals to adjust slowly to the new light cycle. Figure 4a and b shows the actograms as averaged and binned (bin = 1h) homecage activity of CD1 and LAB animals. Figure 4c depicts the overlaid activity of CD1 and LAB animals over entire course of the experiment. CD1 animals showed a pronounced circadian rhythmicity in

their locomotor activity during baseline (days 1+2). By far the greatest portion of activity is observed during the dark phase. With the onset of the light phase this activity ceased. LAB animals on the contrary showed a less contrasted activity profile with high activity at the beginning of the light phase. The overall averaged activity per day (Fig. 4d) of LAB animals was approx. two-times increased compared to CD1 controls and different throughout the experiment ($F_{1,184} = 24.95$, $p < 0.0001$), confirming the hyperactivity phenotype of LAB animals. The light cycle shift (LCS) on day 3 forced the animals to adapt their activity pattern to the new onset of the dark phase. Over the course of days 4-6, both CD1 and LAB animals significantly increased their locomotor activity during the first 6h of the dark phase (Fig. 4e) compared to baseline (CD1: $F_{2,6} = 5.47$, $p = 0.0375$; LAB: $F_{2,6} = 5.92$, $p = 0.0317$), indicating that both strains were able to adjust their circadian locomotor activity. Between 8:00AM and 2:00PM (time point B, unaltered light condition) both strains showed equal amounts of activity ($F_{1,20} = 1.85$, $p = 0.2459$), which was also unaffected by the LCS (Fig. 4f). The locomotor activity at time point C (2:00PM to 8:00PM, now light phase) of CD1 animals at days 5+6 decreased strongly ($F_{2,6} = 13.21$, $p = 0.0047$) indicating a robust photoentraining effect (Fig. 4g). LAB animals on the other hand did not react to the altered light cycle. The modulation of locomotion by light cycle changes became evident when the individual, averaged activity of 3h after a change, was normalized to 3h before and was plotted for every change in cycle (Fig. 4h). During days 1-3 this modulation was prominent for CD1 and LAB mice. After the light cycle shift the modulation was severely disturbed in both strains. While LAB animals seemed to be unable to establish normal rhythmicity in the observed time window, CD1 animals could recover quickly. A strong time effect was revealed by 2-way ANOVA ($F_{9,40} = 50.45$, $p < 0.0001$) with moderate interaction ($F_{9,40} = 2.53$, $p < 0.0212$). This indicates that LAB animals are impaired in using photoentraining signals to adjust their circadian rhythm compared to CD1 controls.

Discussion

Here we have described the design, construction and validation of a simplified microwave-based motion detector for home cage activity monitoring in mice. We have emphasized all necessary steps to copy and built the proposed project. Particular care was taken to use readily available parts in order to ease the straightforward adoption and 'jump-start' the application in the laboratory. We have demonstrated the high detection accuracy and temporal resolution. Moreover, we could show for the first time that animals which were selectively bred for low-anxiety behavior (LAB), a model



organism for extremely low levels of trait anxiety [21] and attention-deficit hyperactivity disorder [22], have strong deficits in photoentrainment.

Deficient photoentrainment in LAB mice

Photoentraining signals reach the retinal ganglion cells (RGC), which constitute the optic tract, and in turn send the photic information from the retina via the retino-hypothalamic tract (RHT) to the two primary targets of the circadian regulatory system, namely the suprachiasmatic nucleus (SCN) and the intergeniculate leaflet of the

the thalamus (IGL) [36]. However, the SCN is considered to act as the ‘master clock’ [37]. Only the photic signals perceived via the eyes carry entraining information, as binocular enucleation completely abolishes photoentrainment [38]. Theories about extraocular photoreception [39] e.g. humoral phototransduction have not been substantiated nor accepted so far [40]. Despite the photoreceptor cells within the retina (rods & cones) also as special form of RGCs have been found to be intrinsically photosensitive (ipRGC) through their photopigment melanopsin. Genetic ablation of these cells was found

to abolish photoentrainment [41, 42] and indicates that visual information via rods and cones is not necessary for functional circadian photoentrainment. This is further substantiated by studies with mice which carry a homozygous mutation in the gene *Pde6b* encoding for the rod-specific phosphodiesterase 6b. These *rd1* mice (retinal degeneration 1) lose their rod photoreceptors within the first weeks after birth, followed by a secondary, slower degeneration of the cone photoreceptor cells [43], leading to complete retinal blindness while RGC function is unaffected. These animals, however, have been shown to exhibit normal circadian rhythms [44]. The LAB mouse line descended from the commonly used outbred strain CD1 which has been described of possessing high incidences of retinal degeneration [45]. Whether LAB animals carry the *rd1* mutation is currently not known, but would otherwise also not explain their deficient circadian photoentrainment. Interestingly there is growing evidence that links ADHD with disturbed sleeping patterns and distorted circadian rhythms [46, 47]. The underlying neurophysiological changes in LAB animals, impairing the ability to entrain their circadian rhythm to photic stimuli, cannot be resolved at this stage. But a potentially altered functionality of the SCN in LAB animals could explain the hyperactivity as well as the previously described altered sleeping patterns [23] and possibly also the impairment in photoentrainment.

Significance of the current design

Several studies so far have proposed elegant ways to monitor activity in small animals like mice and invertebrates. The by far most widely applied methods usually utilize some sort of optical readout, be it (active) infrared light beam crossings [9, 48, 49] or motion detection using passive infrared (PIR) sensors [14], which detect black body radiation in the mid infrared ($\approx 3 \mu\text{m}$) range. These methods are readily applied as their operating principles are easy to comprehend and their technical implementation is rather simple. However all optical based approaches have in common that a constant, unobstructed, visual access must be guaranteed throughout the experiment, and those typically last several days up to weeks. It is therefore desirable to house the animals in their accustomed environment also during home cage activity monitoring in order to minimize distress and long acclimatization periods. With the sanitary and technical advances in animal husbandry, the conventional grid top cages are progressively replaced by individually ventilated cages (IVCs), which are typically operated in specific high-density racks. These systems provide only little space around the cages and obscure most sides especially the top side (filter top). Therefore the usage of microwave based radar systems, which have been beautifully described previously [20, 50, 51], is advisable. However, none of the previously

published studies give detailed building instructions which would be necessary to enable an electronics novice to copy and apply the method. Our design is simple to implement and involves the crucial basic building blocks, like the popular Arduino microcontroller platform and the powerful scientific programming language Python, which form the core of many open-source research equipment projects [52–54]. The decision to favor the Arduino Uno microcontroller board over other devices like the single-board computers Raspberry Pi or the BeagleBone (for a comparison of the different systems see Leccese et al. 2014 [55]) was motivated by the fact that the Arduino platform is an ideal candidate for beginners due to the plethora of available online documentation, while offering more than sufficient peripherals, on-board connectivity features and computing power to fulfill the respective tasks.

There are some additional features which might be desirable to implement in the future which will be briefly mentioned: (1) The measured output is given as activity per minute which is simply the detector activation per minute and an ongoing locomotion triggers the detector several times. For our purpose, this measure was sufficient, but more biologically relevant measures like percent activity over time can be implemented in the Python script. (2) More advanced analysis parameters like period, phase and phase-shift can be obtained from the acquired data and the reader is advised to follow the excellent protocols and guidelines for analyzing locomotor activity rhythms published by Rosato et al. (2006) [56] and Jud et al. (2005) [57]. (3) Instead of storing the data onto a SD card, it is rather simply possible to use an additional WiFi or Ethernet shield to send the data directly to a central network storage or cloud service. Thereby, also the parallel use of several motion detectors at once is realized best. (4) In addition one could equip the microwave based motion detector system with one or several small serial cameras. Thereby, the entire system can be used to e.g. study wildlife animal densities in the field. The Doppler shift sensors consume very little amount of current (6.3 mA) while providing large spatial coverage. A detected motion could be used to wake up the Arduino board from deep sleep, whereby the overall power consumption is minimized enabling even battery powered operation in a reasonable manner.

Potentially hazardous effects of microwave radiation

The FCC rules for the use of radio frequency devices within a building [34] and the established safety standards for general public environments [35] are only valid with respect to the human physiology. It is therefore an important question whether our device, emitting 10.525 GHz, might exert any biological effects on mice. First we try to estimate the emitted power of the microwave radiation. In the data sheet [29] we find the maximal effective isotropic

radiated power (EIRP) of 14 dBm which is equivalent to 25.12 mW radiated power during continuous wave (CW) operation. Therefore we can predict the power density S ($\frac{W}{m^2}$) using the formula $S = \frac{EIRP(W)}{4\pi R^2}$ [58], where R is the distance in meter. This formula over-predicts the power densities in the near-field [58], but can be used for making a ‘worst-case’ or conservative prediction. A mouse is exposed most to the microwaves, if it would build its nest directly in front of the sensor. In our experiments we have mounted the sensor modules 6 cm above the cage floor with double-sided tape directly at the outside of the cages. Considering bedding material and the approximate size of the murine body we therefore assume a minimal distance of 2 cm to the sensor. Given this distance we can estimate a power density of ≈ 0.5 mW/cm². However our module does not emit this power constantly but only at less than 4% of the time, giving an approximate averaged power density of < 0.02 mW/cm².

However there is compelling evidence [59] that microwave (10 Ghz) exposure to infant mice (postnatal day) at a power density of 0.25 mW/cm² for 2 h/day (CW), for 15 consecutive days stresses the animals, as shown by a decreased weight gain and ultimately leads to a decreased performance in a spatial memory task (Morris water maze) later in their live (>6 weeks). Further, 10 Ghz exposure to adolescent (>6 weeks) animals with the same intensity and exposure regime, but for 30 consecutive days also leads to decreased performance in the Morris water maze [60]. However another study showed that constant 10 Ghz exposure in adolescent mice (>4 weeks) at 13 dBm (20 mW) for 6 consecutive days modulated at 8 Hz (within the theta-alpha EEG frequency band) but not at 2 Hz (within the delta EEG frequency band) decreased the spontaneous locomotor behavior in an open-field test. Despite the modulation (assuming 100% amplitude modulation), the effective microwave power (based on the root mean square) used in this study and those mentioned in the studies before, are $> 12\times$ higher (taking the low duty cycle of our sensors into account). Therefore we consider the microwave radiation emitted from the sensor modules used in our design to be nonhazardous for mice.

Conclusion

We have successfully developed a simple, yet powerful open-source tool which aids laboratory practice while reducing costs. It is suitable for the beginner (e.g undergraduate behavioral neuroscience course) but holds enough expandability to satisfy the advanced. Do-it-yourself (DIY) solutions have been considered all too often as a compromise and inferior in performance compared to commercial products. However, knowing the limitations of an own design allows the careful and responsible interpretation of the obtained data, which might

sometimes be better than simply relying entirely on the output of an expensive setup.

Additional file

Additional file 1: Listings. (PDF 69 kb)

Abbreviations

ADC: Analog-to-digital converter; ADHD: Attention deficit hyperactivity disorder; ANOVA: Analysis of variance; DIY: Do-it-yourself; EEG: Electroencephalography; EIRP: Effective isotropic radiated power; GND: Ground; GPIO: General purpose input/outputs; IDE: Integrated development environment; IGL: Intergeniculate leaflet of the thalamus; ipRGC: Intrinsically photosensitive retinal ganglion cell; IVC: Individually ventiated cages; LAB: Low anxiety-related behavior (mice); LCS: Light cycle shift; LED: Light-emitting diode; MDS: Motion detector shield; PCB: Printed circuit board; Pde6b: Phosphodiesterase 6b; PIR: Passive infrared; rd1: Retinal degeneration 1; RGC: Retinal ganglion cell; RHT: Retinohypothalamic tract; RTC: Real-time clock; SCN: Suprachiasmatic nucleus; SMD: Surface-mounted device

Acknowledgements

Not applicable.

Funding

Not applicable.

Availability of data and materials

All design files and original data which has been used to prepare the figures are available online [25] or on request.

Authors' contributions

AG conceived the idea for the study, designed and built the MDS, wrote the Arduino and Python scripts, performed and analyzed the experiments and wrote the manuscript and designed all figures and graphical representations. DEH, PMK and KK participated in the experiments. CTW performed part of the statistical analysis and wrote on the manuscript. All authors read and approved the final manuscript.

Ethics approval and consent to participate

Experimental procedures involving animals were approved (AZ 188-12) by the Committee on Animal Health and Welfare of the State of Bavaria (Regierung von Oberbayern, Munich, Germany). Animal care taking and experiments were performed in compliance with the European Economic Community (EEC) directive on the protection of animals used for scientific purposes (2010/63/EU).

Consent for publication

Not applicable.

Competing interests

The authors declare that they have no competing interests.

Publisher's Note

Springer Nature remains neutral with regard to jurisdictional claims in published maps and institutional affiliations.

Author details

¹Max Planck Institute of Psychiatry, Dep. Stress Neurobiology and Neurogenetics, RG Neuronal Plasticity, Kraepelinstr. 2-10, D-80804 Munich, Germany. ²Neuroscience Master's Program, Interdisciplinary Center for Neurosciences (IZN), Heidelberg University, Im Neuenheimer Feld 504, D-69120 Heidelberg, Germany. ³Department of Psychiatry and Psychotherapy, Ludwigs-Maximilians-University, Nußbaumstraße 7, D-80336 Munich, Germany. ⁴Fresenius University, Infanteriestraße 11a, D-80797 Munich, Germany. ⁵Institute of Applied Physiology, Ulm University, Albert-Einstein-Allee 11, N26/4406, D-89081 Ulm, Germany.

Received: 28 June 2017 Accepted: 29 August 2017

Published online: 16 November 2017

References

- McClung C. How might circadian rhythms control mood? let me count the ways. *Biol Psychiatry*. 2013;74(4):242–9.
- Belzung C, Lemoine M. Criteria of validity for animal models of psychiatric disorders: focus on anxiety disorders and depression. *Biol Mood Anxiety Disord*. 2011;1(1):9. doi:10.1186/2045-5380-1-9.
- Griesauer I, Diao W, Ronovsky M, Elbau I, Sartori S, Singewald N, Pollak D. Circadian abnormalities in a mouse model of high trait anxiety and depression. *Ann Med*. 2014;46(3):148–54.
- Bartlang M, Oster H, Helfrich-Förster C. Repeated psychosocial stress at night affects the circadian activity rhythm of male mice. *J Biol Rhythm*. 2015;30(3):228–41.
- Palidwor G, Andrade-Navarro M. MLTrends: Graphing MEDLINE term usage over time. *J Biomed Discov Collab*. 2010;5:1–6.
- Parreño A, Sarazá M, Subero C. A new stabilimeter for small laboratory animals. *Physiol Behav*. 1985;34(3):475–8.
- Megens A, Voeten J, Rombouts J, Meert T, Niemegeers C. Behavioral activity of rats measured by a new method based on the piezo-electric principle. *Psychopharmacol (Berl)*. 1987;93(3):382–8.
- Ganea K, Liebl C, Sterlemann V, Müller M, Schmidt M. Pharmacological validation of a novel home cage activity counter in mice. *J Neurosci Methods*. 2007;162(1-2):180–6.
- Clarke RL, Smith RF, Justesen DR. An infrared device for detecting locomotor activity. *Behav Res Methods Instrum Comput*. 1985;17(5):519–25.
- Tarpy RM, Murcek RJ. An electronic device for detecting activity in caged rodents. *Behav Res Methods Instrum Comput*. 1984;16(4):383–7.
- Stoff D, Stauderman K, Wyatt R. The time and space machine: continuous measurement of drug-induced behavior patterns in the rat. *Psychopharmacol (Berl)*. 1983;80(4):319–24.
- Morrel-Samuels P, Krauss R. Cartesian analysis: A computer-video interface for measuring motion without physical contact. *Behav Res Methods Instrum Comput*. 1990;22(5):466–70.
- Banks G, Nolan P. Assessment of Circadian and Light-Entrainable Parameters in Mice Using Wheel-Running Activity. *Curr Protoc Mouse Biol*. 2011;1(3):369–81.
- Tamborini P, Sigg H, Zbinden G. Quantitative analysis of rat activity in the home cage by infrared monitoring. application to the acute toxicity testing of acetanilide and phenylmercuric acetate. *Arch Toxicol*. 1989;63(2):85–96.
- Young C, Young M, Li Y, Lin M. A new ultrasonic method for measuring minute motion activities of rats. *J Neurosci Methods*. 1996;70(1):45–9.
- Marsden C, King B. The use of Doppler shift radar to monitor physiological and drug induced activity patterns in the rat. *Pharmacol Biochem Behav*. 1979;10(5):631–5.
- Vanuytven M, Vermeire J, Niemegeers C. A new motility meter based on the Doppler principle. *Psychopharmacol (Berl)*. 1979;64(3):333–6.
- Martin PH, Unwin DM. A microwave doppler radar activity monitor. *Behav Res Methods Instrum Comput*. 1980;12(5):517–20.
- Rose F, Dell P, Love S. Doppler shift radar monitoring of activity of rats in a behavioural test situation. *Physiol Behav*. 1985;35(1):85–7.
- Pasquali V, Scannapieco E, Renzi P. Validation of a microwave radar system for the monitoring of locomotor activity in mice. *J Circadian Rhythm*. 2006;4(7). doi:10.1186/1740-3391-4-7.
- Krömer SA, Keßler MS, Milfay C, Birg IN, Bunck M, Czibere L, Panhuysen M, Pütz B, Deussing JM, Holsboer F, Landgraf R, Turck CW. Identification of Glyoxalase-I as a Protein Marker in a Mouse Model of Extremes in Trait Anxiety. *J Neurosci*. 2005;25(17):4375–84.
- Yen YC, Anderzhanova E, Bunck M, Schuller J, Landgraf R, Wotjak CT. Co-segregation of hyperactivity, active coping styles, and cognitive dysfunction in mice selectively bred for low levels of anxiety. *Front Behav Neurosci*. 2013;7(103). doi:10.3389/fnbeh.2013.00103.
- Jakubcakova V, Flachskamm C, Landgraf R, Kimura M, Quitkin F. Sleep Phenotyping in a Mouse Model of Extreme Trait Anxiety. *PLoS ONE*. 2012;7(7):e40625. doi:10.1371/journal.pone.0040625.
- KiCad EDA. A Cross Platform and Open Source Electronics Design Automation Suite. <http://kicad-pcb.org>. Accessed 05 June 2017.
- Resources for the Motion Detector Shield. doi:10.5281/zenodo.848280 <https://github.com/AGenews/MDS/tree/v0.4>. Accessed 05 June 2017.
- Park OSH. An Electric Ecosystem. <https://oshpark.com>. Accessed 05 June 2017.
- Arduino IDE. <https://www.arduino.cc/en/main/software>. Accessed 05 June 2017.
- Continuum Analytics, Anaconda Software Distribution. <https://continuum.io/>. Accessed 05 June 2017.
- Parallax Inc., X-Band Motion Detector (32213). v1.1. https://www.parallax.com/sites/default/files/downloads/32213-X-BandMotionDetector-v1.1_0.pdf. Accessed 05 June 2017.
- Lucas RJ, Douglas RH, Foster RG. Characterization of an ocular photopigment capable of driving pupillary constriction in mice. *Nat Neurosci*. 2001;4(6):621–6.
- Jacobs GH, Fenwick JA, Williams GA. Cone-based vision of rats for ultraviolet and visible lights. *J Exp Biol*. 2001;204(Pt 14):2439–46.
- Imai H, Kefalov V, Sakurai K, Chisaka O, Ueda Y, Onishi A, Morizumi T, Fu Y, Ichikawa K, Nakatani K, Honda Y, Chen J, Yau KW, Shichida Y. Molecular properties of rhodopsin and rod function. *J Biol Chem*. 2007;282(9):6677–84.
- Getting Started with Arduino and Genuino Products. <https://www.arduino.cc/en/Guide/HomePage>. Accessed 05 June 2017.
- Federal Communications Commission. Operation within the bands 902-928 MHz, 2435-2465 MHz, 5785-5815 MHz, 10500-10550 MHz, AND 24075-24175 MHz. 2011; 47 CFR 15.245.
- Institute of Electrical and Electronic Engineers (IEEE). Standard for Safety Levels with Respect to Human Exposure to Radio Frequency Electromagnetic Fields, 3 kHz to 300 GHz. 1991; Std C95.1-1991.
- Provencio I, Cooper HM, Foster RG. Retinal projections in mice with inherited retinal degeneration: Implications for circadian photoentrainment. *J Comp Neurol*. 1998;395(4):417–39.
- Moore RY, Speh JC, Patrick Card J. The retinohypothalamic tract originates from a distinct subset of retinal ganglion cells. *J Comp Neurol*. 1995;352(3):351–66.
- Nelson RJ, Zucker I. Absence of extraocular photoreception in diurnal and nocturnal rodents exposed to direct sunlight. *Comp Biochem Phys A*. 1981;69(1):145–8.
- Campbell SS, Murphy PJ. Extraocular Circadian Phototransduction in Humans. *Science*. 1998;279(5349):396–9.
- Foster RG. Shedding Light on the Biological Clock. *Neuron*. 1998;20(5):829–32.
- Güler AD, Ecker JL, Lall GS, Haq S, Altimus CM, Liao HW, Barnard AR, Cahill H, Badea TC, Zhao H, Hankins MW, Berson DM, Lucas RJ, Yau KW, Hattar S. Melanopsin cells are the principal conduits for rod-cone input to non-image-forming vision. *Nature*. 2008;453(7191):102–5.
- Hatori M, Le H, Vollmers C, Keding SR, Tanaka N, Schmedt C, Jegla T, Panda S, Jegla T, Panda S. Inducible Ablation of Melanopsin-Expressing Retinal Ganglion Cells Reveals Their Central Role in Non-Image Forming Visual Responses. *PLoS ONE*. 2008;3(6):e2451.
- Farber DB, Flannery JG, Bowes-Rickman C. The rd mouse story: Seventy years of research on an animal model of inherited retinal degeneration. *Prog Retin Eye Res*. 1994;13(1):31–64.
- Foster RG, Provencio I, Hudson D, Fiske S, De Grip W, Menaker M. Circadian photoreception in the retinally degenerate mouse (rd/rd). *J Comp Physiol A*. 1991;169(1):39–50.
- Serfilippi LM, Pallman DRS, Gruebbel MM, Kern TJ, Spainhour CB. Assessment of retinal degeneration in outbred albino mice. *Comp Med*. 2004;54(1):69–76.
- Walters AS, Silvestri R, Zucconi M, Chandrashekariah R, Konofal E. Review of the possible relationship and hypothetical links between attention deficit hyperactivity disorder (ADHD) and the simple sleep related movement disorders, parasomnias, hypersomnias, and circadian rhythm disorders. *J Clin Sleep Med*. 2008;4(6):591–600.
- Baird AL, Coogan AN, Siddiqui A, Donev RM, Thome J. Adult attention-deficit hyperactivity disorder is associated with alterations in circadian rhythms at the behavioural, endocrine and molecular levels. *Mol Psychiatry*. 2012;17(10):988–5.
- Pasquali V, Gualtieri R, D'Alessandro G, Granberg M, Hazlerigg D, Cagnetti M, Leccese F. Monitoring and Analyzing of Circadian and Ultradian Locomotor Activity Based on Raspberry-Pi. *Electron (Switzerland)*. 2016;5(3):58. doi:10.3390/electronics5030058.
- Pasquali V, D'Alessandro G, Gualtieri R, Leccese F. A new Data Logger based on Raspberry-Pi for Arctic *Notostraca* Locomotion Investigations. *Measurement*. 2017;110:249–56.

50. Pasquali V, Renzi P. On the use of microwave radar devices in chronobiology studies: An application with *Periplaneta americana*. *Behav Res Meth*. 2005;37(3):522–27.
51. Pasquali V, Capasso A, Renzi P. Circadian and ultradian rhythms in locomotory activity of inbred strains of mice. *Biol Rhythm Res*. 2010;41(1): 63–74.
52. Pearce JM. Materials science. Building research equipment with free, open-source hardware. *Science*. 2012;337(6100):1303–4.
53. Teikari P, Najjar RP, Malkki H, Knoblauch K, Dumortier D, Gronfier C, Cooper HM. An inexpensive Arduino-based LED stimulator system for vision research. *J Neurosci Meth*. 2012;211(2):227–36.
54. Sheinin A, Lavi A, Michaelevski I. StimDuino: An Arduino-based electrophysiological stimulus isolator. *J Neurosci Meth*. 2015;243:8–17.
55. Leccese F, Cagnetti M, Trinca DA. A smart city application: A fully controlled street lighting isle based on Raspberry-Pi card, a ZigBee sensor network and WiMAX. *Sensors (Switzerland)*. 2014;12(14):24408–4.
56. Rosato E, Kyriacou CP. Analysis of locomotor activity rhythms in *Drosophila*. *Nat Protoc*. 2006;1(2):559–68.
57. Jud C, Schmutz I, Hampp G, Oster H, Albrecht U. A guideline for analyzing circadian wheel-running behavior in rodents under different lighting conditions. *Biol Proced Online*. 2005;7(1):101–16.
58. Federal Communications Commission. Evaluating Compliance with FCC Guidelines for Human Exposure to Radiofrequency Electromagnetic Fields. Supplement C to OET bulletin. 1997; Supplement C to OET bulletin 65 (Edition 97-01).
59. Sharma A, Kesari KK, Saxena VK, Sisodia R. Ten gigahertz microwave radiation impairs spatial memory, enzymes activity, and histopathology of developing mice brain. *Mol Cell Biochem*. 2017. doi:10.1007/s11010-017-3051-8. [Epub ahead of print].
60. Sharma A, Sisodia R, Bhatnagar D, Saxena VK. Spatial memory and learning performance and its relationship to protein synthesis of Swiss albino mice exposed to 10 GHz microwaves. *Int J Radiat Biol*. 2014;90(1): 29–35.

Submit your next manuscript to BioMed Central and we will help you at every step:

- We accept pre-submission inquiries
- Our selector tool helps you to find the most relevant journal
- We provide round the clock customer support
- Convenient online submission
- Thorough peer review
- Inclusion in PubMed and all major indexing services
- Maximum visibility for your research

Submit your manuscript at
www.biomedcentral.com/submit

